



HAL
open science

A novel approach combining thermosiphon and phase change materials (PCM) for cold energy storage in cooling systems

Maria Aurely Yedmel, Romuald Hunlede, Stéphanie O.L. Lacour, Graciela Alvarez, Anthony Delahaye, Denis Leducq

► To cite this version:

Maria Aurely Yedmel, Romuald Hunlede, Stéphanie O.L. Lacour, Graciela Alvarez, Anthony Delahaye, et al.. A novel approach combining thermosiphon and phase change materials (PCM) for cold energy storage in cooling systems. International Journal of Refrigeration, inPress, 10.1016/j.ijrefrig.2023.12.015 . hal-04346393

HAL Id: hal-04346393

<https://hal.inrae.fr/hal-04346393>

Submitted on 15 Dec 2023

HAL is a multi-disciplinary open access archive for the deposit and dissemination of scientific research documents, whether they are published or not. The documents may come from teaching and research institutions in France or abroad, or from public or private research centers.

L'archive ouverte pluridisciplinaire **HAL**, est destinée au dépôt et à la diffusion de documents scientifiques de niveau recherche, publiés ou non, émanant des établissements d'enseignement et de recherche français ou étrangers, des laboratoires publics ou privés.

A novel approach combining thermosiphon and phase change materials (PCMs) for cold energy storage in cooling systems

Maria Aurely Yedmel^(a), Romuald Hunlede^(a), Stéphanie Lacour^(a), Graciela Alvarez^(a), Anthony Delahaye^(a), Denis Leducq^{*(a)}

^(a)Université Paris-Saclay, INRAE, FRISE, 92761 Antony, France

*Corresponding author: denis.leducq@inrae.fr

ABSTRACT

A novel approach combining thermal energy storage (TES) and a thermosiphon was investigated for cold storage. The use of TES units for cooling systems has been studied for many years, as they are well suited for short-term energy storage. A cold latent heat accumulator was designed to replace the function of any vapour compression cycle in the event of electrical failure without using any electrical device but rather the thermosiphon principle. A laboratory prototype of a thermosiphon combined with the cold accumulator was developed using a paraffin mixture as a phase change material (PCM). The accumulator was connected to the vapour compression system of a closed display cabinet. An experimental study was carried out by simulating 1.5-hour compressor shutdowns with and without the accumulator. The air and product temperatures in the cabinet, the behaviour of the compressor during restart, and the charging and discharging processes of the accumulator were analysed. The results showed that shutting down the compressor with the cold accumulator significantly reduces the increase of air and product temperatures compared to shutting down without the accumulator. The air temperature in the rear duct was maintained within the acceptable temperature range for 72 minutes with the accumulator, compared to 3 minutes without. A default in the design of the accumulator was observed during the charging phase, as some areas of

24 the accumulator never reached 80 % of charge. This new approach extends demand-side
25 management and renewable energies to all end users of vapour compression machines.

26 Refrigeration, Cold storage, Thermosiphon, PCM, Power outages, Demand-side management

27

28 **1. Introduction**

29 Cooling systems are used to maintain or reduce the temperature of a fluid or a solid to a lower level.
30 Typically, a refrigerant circulates through a vapour compression cycle where it removes heat from
31 the cold source and transfers it to the hot source. Vapour compression systems are used for
32 refrigeration (domestic, commercial, industrial, and transport refrigeration) and air conditioning
33 (room and mobile air conditioning) (Dong et al., 2021) and are very energy intensive. Dupont et al.
34 (2019) state that the refrigeration sector accounts for about 20 % of global electricity consumption.
35 In 2018, 20 % of this share was attributable to electric fans and air conditioners installed in buildings
36 (IEA, 2018). In addition, in industrialised countries, 30-60 % of the electricity consumed by
37 supermarkets is due to refrigeration systems (UNIDO, 2020). In the context of global warming,
38 several measures have been implemented to reduce the electricity consumption of vapour
39 compression systems. One of these methods is to use thermal energy storage (TES) technologies to
40 store thermochemical, latent, or sensible heat for later use and facilitate the use of intermittent
41 renewable energy sources.

42 In the case of latent heat storage, phase change materials (PCMs) are used as the medium. PCMs can
43 store heat or cold by changing phase, for example, from liquid to solid, and release this energy by
44 changing phase as well, but in reverse, from solid to liquid. Phase change occurs at a temperature
45 called the phase change temperature (T_{pc}), which depends on the operating pressure and predefines
46 the application of the PCM. PCMs can be organic compounds (paraffin/non-paraffin), inorganic
47 compounds (salt hydrate/metal), or eutectic compounds (organic-organic, inorganic-inorganic, and

48 organic-inorganic). Some benefits of organic PCMs are their chemical inertia, recyclability, low
49 vapour pressure in the melt form, and small volume change during phase transition. Their low
50 thermal conductivity and incompatibility with plastic containers are some disadvantages. Inorganic
51 PCMs and mostly salt hydrates can be preferred for their availability, non-flammability, high latent
52 heat of fusion, and high thermal conductivity. However, they are corrosive, irritant, and have high
53 vapour pressure.(Memon, 2014)

54 PCMs can be added to building materials to reduce indoor temperature fluctuations and thus the
55 energy consumption of air conditioning systems without increasing the structure' mass (Socaciu et
56 al., 2014) (Memon, 2014). Hawes et al. (1989) studied the use of PCMS in concrete to store latent
57 heat and found that among three different PCMs, DODECANOL (T_{pc} : 21 °C) was the one that was
58 compatible with both autoclaved concrete blocks and ordinary concrete blocks. Wang et al. (2022)
59 successfully combined wild daisy flower stems with paraffin to obtain a stable composite (T_{pc} : 40.1
60 °C) capable of regulating the temperature of a building by acting as a thermal buffer. In the
61 refrigeration domain, PCMs can help to maintain product temperature and replace the cold machine
62 during a given period. They are, therefore, massively studied in the literature to be used in insulated
63 boxes, refrigerated trucks, domestic refrigerators, display cabinets, and cold storage facilities
64 (Leungtongkum et al., 2022). In these studies, the PCM configuration (PCM melting point, quantity,
65 position...) and the operating conditions (refrigerant temperature, ambient temperature, insulation
66 material...) are crucial parameters. Ahmed et al. (2010) examined the effects of incorporating
67 paraffin (T_{pc} : 5 °C) into the insulation system of a refrigerated truck and observed that it reduced
68 heat transfer and temperature fluctuations by 16.3 %. Liu et al. (2012) proposed a new refrigeration
69 system with inorganic salt (T_{pc} : -30.6 °C) inside the refrigerated truck and the refrigeration unit
70 placed outside. The new system reduced energy costs by 50 % and maintained the truck's
71 temperature at -18 °C for 10 hours in extreme weather conditions (T_{pc} : 41 °C). Oró et al. (2012)
72 studied the integration of Climsel (T_{pc} : -18 °C) in a vertical freezer and found that during a 3-hour
73 power failure, the air and product temperature increased less with the PCM than without (6 °C less

74 and 2 °C less, respectively). Azzouz et al. (2009) placed water (T_{pc} : 0 °C) on the back of the
75 evaporator of a domestic refrigerator, increasing its coefficient of performance (COP) by 10-30 % and
76 allowing continuous operation for 5-6 hours without electricity. Additionally, Maiorino et al. (2019)
77 utilised water as PCM placed on top and bottom of refrigerator shelves. Compared to a 3.1 °C
78 temperature difference between two shelves without PCM, 0.2 °C was observed with PCM.

79 About display cabinets, fewer works were reported in the literature. Alzuwaid et al. (2015) placed
80 heat exchanger with water gel (T_{pc} : -2 °C) in the rear channelling of an open-door refrigerated
81 display cabinet. Temperatures in the products were homogenised, the compressor running time was
82 decreased, and the maximum air temperature was reduced by 2 °C. Water (T_{pc} : 0 °C) was also
83 integrated into an open-door display cabinet (Ben-Abdallah et al., 2019). During 2 hours of
84 compressor downtime, products temperature increased by 1 °C, with the PCM heat exchanger,
85 compared to 2 °C without the PCM heat exchanger. However, adding the heat exchanger without
86 PCM in the rear duct decreased the air velocities at the discharge air grid (-28 % air curtain flowrate)
87 and the fifth shelf. This decrease in air velocity results in higher product temperatures at the front
88 and fifth shelves than without the heat exchanger (for example, from 4.4 °C without the heat
89 exchanger to 7.9 °C with the heat exchanger). Ben-Abdallah et al. (2019) confirmed that the position
90 of the PCM in the refrigerated display cabinet is essential to avoid any unwanted melting or
91 obstruction of the cold air passage.

92 Thermosiphon technology shows high potential to fully utilise PCM potential without obstructing
93 airflow since the proximity between the PCM and the evaporator is not required anymore.
94 Thermosiphon effect is driven by the natural circulation of fluids due to the difference in density. It
95 requires no electrical or mechanical components to move the fluid, thus saving energy. Many
96 researchers have recently proposed to optimise cooling systems using thermosiphon technology. Lee
97 et al. (2009) designed a hybrid cooler capable of operating in both vapour compression and
98 thermosiphon modes depending on the ambient temperature. In the nuclear sector, the

99 thermosiphon loop is considered as an efficient and reliable long-term cooling system for the spent
100 fuel pool (Ye et al., 2013) (Fu et al., 2015) (Trewin, 2021). Li et al. (2018) investigated a two-phase
101 thermosiphon loop to cool a motorised spindle shaft and observed improved heat transfer
102 performance. Sutanto et al. (2022) integrated thermosiphon in a floating photovoltaic (PV) system
103 and noted an increase of 7.86 % in the panels' power output compared to ground PV and an increase
104 of 3.34 % compared to floating PV without thermosiphon.

105 For refrigeration systems, two-phase loop thermosiphons were studied to characterise the fluid flow
106 and to understand the effects of operating parameters on its performance (Zhang et al., 2015)
107 (Albertsen and Schmitz, 2021) (Wang et al., 2023). Coupled with PCM, thermosiphon can be used as
108 a new energy-efficient optimisation technology for cooling systems. FOSTER et al. (2013) and Foster
109 et al. (2015) compared the use of electricity to the use of a thermosiphon coupled with PCM for
110 display cabinet defrosting. The thermosiphon melted the frost faster than the electric defrosting and
111 reduced the total energy consumption of the cabinet. Liu et al. (2021) investigated the capacity of a
112 two-phase loop thermosiphon to accurately regulate the temperature of the fresh food
113 compartment of a modified refrigerator. The loop was coupled to a PCM (mixture of NaCl, C₃H₈O₃,
114 and H₂O), located in the freezer, to provide cooling to the fresh food section. The system was
115 successful in regulating the temperature of the compartment.

116 This paper aims to present the working principle of a novel thermal energy storage device combining
117 PCM and thermosiphon technologies. The accumulator is designed to replace the cooling machine
118 during voluntary or involuntary power outages in order to reduce energy consumption and enhance
119 the implementation of renewable energy and demand-side management. The originality of the
120 accumulator lies in the fact that it can be plugged into any current vapour compression cycle without
121 the need for a secondary fluid or an atypical/additional cooling system and without obstructing the
122 airflow or any other part of the existing system. The characteristics of the accumulator and its
123 functioning when inserted into the vapour compression cycle of the equipment are detailed in the

124 paper. The accumulator was tested in a closed-door instrumented refrigerated display cabinet. The
125 changes in air and product temperatures during a 2-hour demand side management (compressor
126 shutdown) with and without the accumulator are presented.

127

128 **2. Material and methods**

129 **2.1 Accumulator description and integration in a vapour compression cycle**

130 2.1.1 Cold storage accumulator design

131 A vapour compression machine has four main components: an expansion valve, an evaporator, a
132 compressor, and a condenser. As the refrigerant passes through the loop, it undergoes multiple
133 compression and expansion cycles, producing continuous cooling by absorbing heat from the
134 evaporator and rejecting it to the surrounding environment through the condenser. Thermal energy
135 storage can be achieved either by convective exchange with cold air, by direct contact of the material
136 with the evaporator, or by using a secondary fluid. Placing the PCM in the cold air stream produced
137 at the evaporator encroaches on the volume dedicated to storage, thus limiting the amount of PCM
138 or product stored. When applied in contact with the evaporator, the PCM can also impinge on
139 airflow (Ben-Abdallah et al., 2019) and reduce the exchange surface of the evaporator, thus
140 decreasing its performance. Besides, there is no control over the charge and discharge periods of the
141 PCM due to compressor shutdown cycles. The most common method is to use a secondary
142 refrigerant to transport the cold from the evaporator to a remote storage unit and return it when
143 needed. However, this involves two levels of heat exchange, which reduce the thermodynamic
144 efficiency of the system and increase energy consumption and cost.

145 The novel system controls charging and discharging phases without a secondary refrigerant and
146 therefore has better thermodynamic efficiency. The PCM is placed in a container with a finned tube
147 heat exchanger, and this unit (accumulator) is well insulated with foam rubber to limit heat exchange

148 with the surrounding environment. During the charging phase, thermal energy is stored in the
149 accumulator while the refrigerating machine is running by direct exchange between the PCM and the
150 refrigerant circulating in the copper tubes. The charging phase must be fast so that the accumulator
151 can be charged at any time and the cooling machine can be replaced in case of need. The aluminium
152 fins of the heat exchanger increase the exchange surface between the PCM and the refrigerant,
153 which increases the efficiency of heat transfer. During the discharging phase (in the absence of
154 electricity), the cold is returned to the evaporator by the thermosiphon effect. This stored cold
155 energy must be able to meet the thermal load requirements at the evaporator. For this, the
156 properties of the chosen PCM are crucial in determining the required volume of the accumulator and
157 thus the amount of energy available during discharging phase. This charging and discharging principle
158 is independent of the evaporator technology used by the machine. An additional system for a second
159 refrigerant loop is not required, which reduces the cost. The accumulator can be placed outside the
160 cold chamber, and thus does not occupy the space foreseen for the refrigerated products.

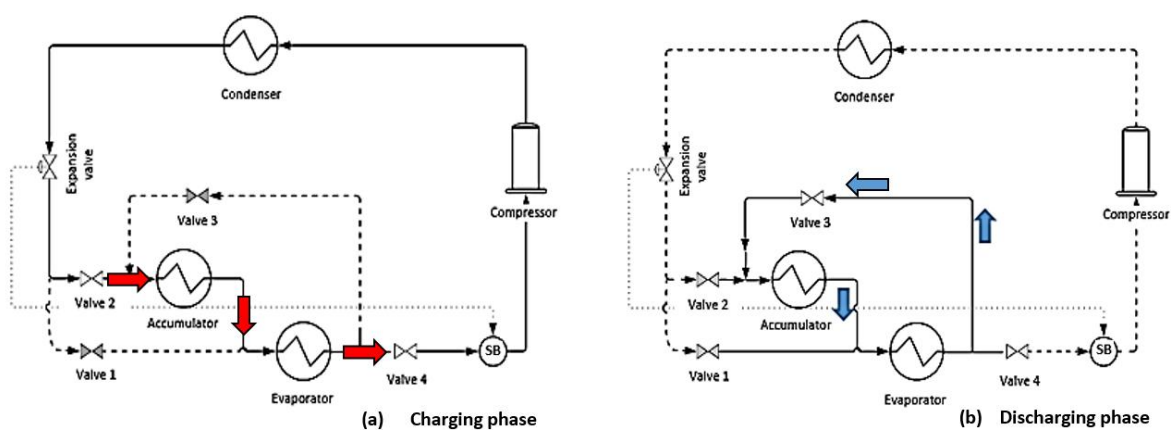
161

162 2.1.2 Cold storage accumulator integration and thermosiphon loop

163 Figure 1 shows the insertion of the accumulator in the vapour compression cycle. The accumulator is
164 connected to the loop at the evaporator inlet. A set of controllable valves (V1-V4) is used to control
165 the charge and discharge of the accumulator. The cooling circuit also includes a thermostatic
166 expansion valve (TXV) to maintain a satisfactory refrigerant level in the evaporator. Valves 1 and 3
167 are closed during the charging phase; while valves 2 and 4 are open (Figure 1.a). The refrigerant
168 leaves the thermostatic expansion valve and enters the accumulator, where it transfers cold energy
169 to the PCM. The PCM drops in temperature and solidifies, while the refrigerant partially evaporates.
170 The refrigerant then finishes exchanging thermal energy when it passes through the evaporator and
171 leaves it as vapour. Therefore, when the PCM is completely solid, all the energy carried by the
172 refrigerant is transferred to the evaporator.

173 In the discharging phase (power cuts), valves 1, 2, and 4 are closed while valve 3 is open, creating a
 174 closed circuit between the evaporator and the accumulator (Figure 1.b). In the evaporator, the liquid
 175 refrigerant absorbs heat from the element to be cooled (through heat exchange with air) and then
 176 evaporates. As a result of the pressure difference between the evaporator and the accumulator (in
 177 the vertical duct), a refrigerant flow due to thermosiphon effect takes place, and the vapour rises
 178 towards the accumulator. The refrigerant in vapour form condenses by absorbing the cold energy
 179 previously stored in the PCM. The refrigerant in liquid form flows back to the evaporator due to
 180 gravity forces, and the cycle is repeated. The PCM gradually heats up until it becomes totally liquid.
 181 At that point, there is no longer enough energy in the PCM to cool down the refrigerant to its liquid
 182 form. The refrigerant stays in its vapour state and is no longer recirculated.

183 The thermosiphon allows the system to operate at around 7 % of the power consumption when the
 184 compressor is on. The evaporator fan is still functioning to enable heat transfer between the
 185 refrigerant and air. Charging and discharging efficiencies are influenced by the height difference
 186 between the accumulator and the evaporator, since gravity is the driving force. An increase in height
 187 difference therefore leads to an increase in thermosiphon performance. However, after a critical
 188 height, the increase in vapour pressure drop can reduce its performance (Lee et al., 2009).



189
 190 *Figure 1. Diagram of the cold storage accumulator integrated into a vapour compression cycle during charging phase (a)*
 191 *and discharging phase (b)*

192 **2.2 Experimental setup and methods**

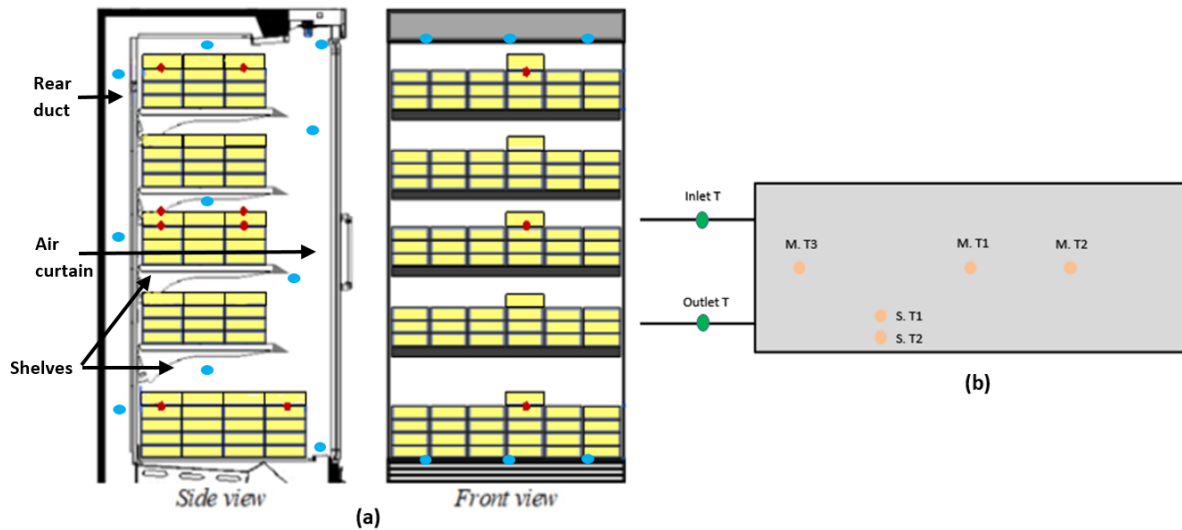
193 2.2.1 Integration of the accumulator in a display cabinet

194 The accumulator (92 x 11 x 26 cm) was integrated into the original vapour compression system of a
195 commercial closed vertical refrigerated display cabinet (OFFLIP 2 Eco DV; 200 x 134.5 x 70.5 cm). The
196 accumulator was located outside the cabinet, in the upper rear part. The height of the riser (OD: 12.7
197 mm; ID: 10.9 mm) and downcomer (OD: 12.7 mm; ID: 10.9 mm) is 152 cm and 125 cm respectively.
198 The display cabinet was a ventilated plug-in cabinet with positive cold storage (0/+2 °C). The PCM
199 used is a chemically inert liquid paraffin mixture (RUBITHERM RT-4) with a phase change
200 temperature T_{pc} from -4 °C to -7 °C, a liquid density of 0.76 kg/l at 15 °C and a storage capacity of
201 180 kJ/kg \pm 7.5 %. About 20 kg of PCM was used for the experiment.

202 2.2.2 Display cabinet and accumulator instrumentation

203 The display cabinet and the accumulator were equipped with calibrated T-type thermocouples
204 (uncertainty of \pm 0.1 °C) (Figure 2). The air temperature was monitored in the rear duct, on the
205 shelves, at the discharge air grid, and at the air curtain using 14 sensors. The display cabinet was
206 loaded with methylcellulose packages (20 x 10 x 5 cm) to simulate food products. About 90 % of the
207 storage volume was occupied in order to simulate a fully loaded display cabinet. The first 4 shelves
208 had 3 columns of products in depth, and the fifth shelf had 4 columns. All the shelves had 6 rows of
209 products of different heights in width. The temperature of the products (core and surface) was
210 measured using 8 sensors. A total of 5 sensors were used to measure the temperature of the PCM in
211 the accumulator. Two additional sensors measured the temperature of the refrigerant at the inlet
212 and outlet of the accumulator. The compressor and condenser of the refrigeration system were also
213 instrumented to evaluate the energy consumption of the display cabinet. Two temperature sensors
214 were placed at the compressor inlet and outlet, and one was used at the condenser outlet. Two
215 pressure sensors were also placed at the compressor inlet and outlet. A Wattmeter was used to
216 measure the power consumed by the cabinet: compressor, fan, and lighting. The tests were carried

217 out in a temperature-controlled room, and the room temperature was monitored. The
218 measurements were recorded using a data acquisition system (Agilent 34970A) at an interval of 10 s
219 after the start of the tests.



220

221 *Figure 2. Illustration of thermocouple arrangement for temperature measurements of air and product (a); PCM and*
222 *refrigerant (b)*

223 2.2.3 Test protocol

224 The test was conducted in a temperature-controlled chamber at 17 °C (± 0.7 °C). The temperature of
225 the cabinet thermostat was set to -3 °C and the doors remained closed for the experiment. Before
226 starting the experiment, the closed display cabinet was run for 24 hours in charging mode to ensure
227 that the PCM was fully charged and that the system reached a steady state.

228 When the systems reached stability, the compressor was shut down twice for 1.5 hours to check the
229 ability of the accumulator to replace the refrigeration system using the thermosiphon principle.

230 During the first shutdown, the system was put into discharging mode using the control valves. Thus,
231 the accumulator was able to supply cold to the display cabinet. For comparison purposes, during the

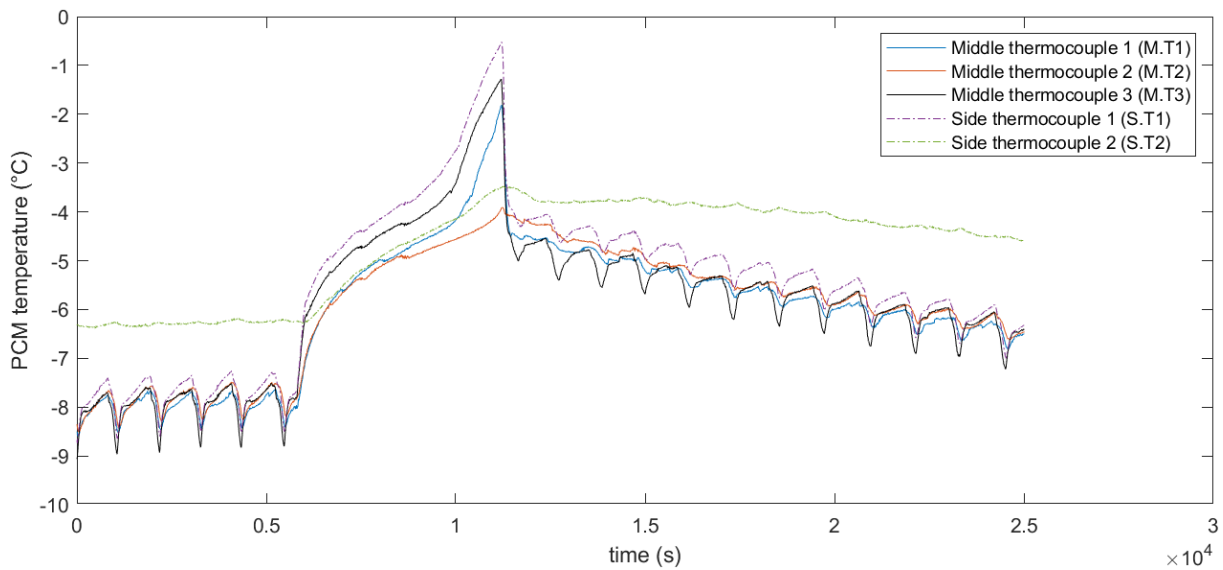
232 second shutdown, the system was operated without the accumulator by closing valves 2 and 3
233 (Figure 1).

234

235 3. Results and discussion

236 3.1 Accumulator charging and discharging processes

237 The charging rate of the accumulator was determined by using the enthalpy versus temperature
238 curve. It allows the determination the amount of energy absorbed from the temperature of the PCM.
239 The 5 thermocouples (3 middle thermocouples and 2-sided thermocouples) placed in the
240 accumulator allow to know the state (solid or liquid) of each designated portion of PCM and thus the
241 state of charge of each portion. The overall charging rate of the accumulator is estimated by taking
242 the arithmetic average of the charging rate of each area. Figure 3 shows the evolution of the
243 temperature of the PCM in the accumulator and Figure 4 presents the evolution of the accumulator
244 charging rate per area during the first shutdown (discharging).

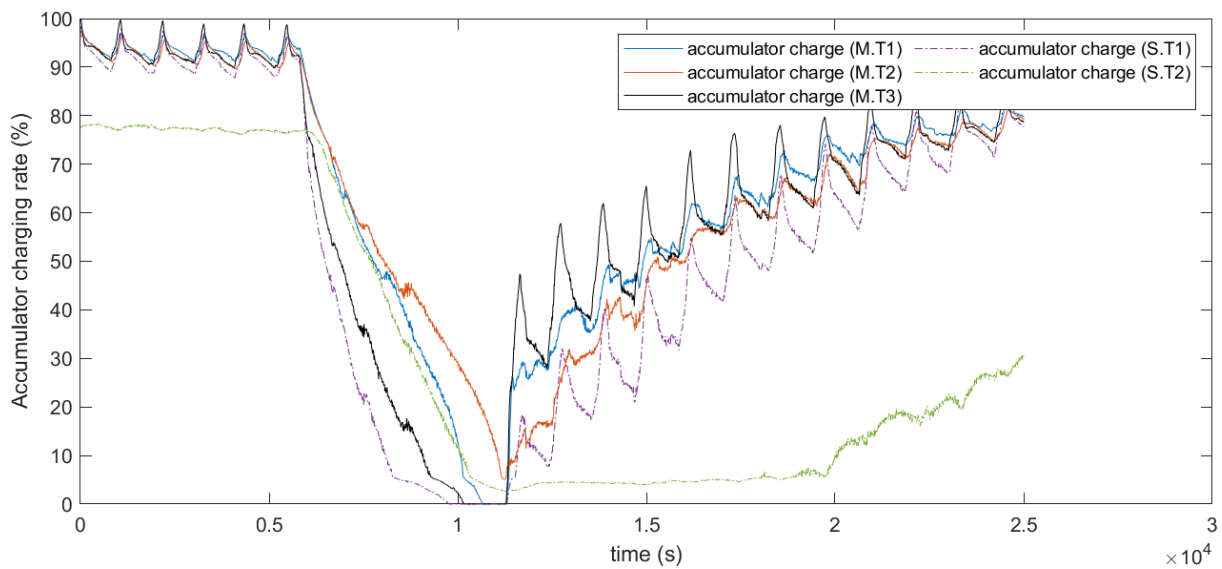


245

246 *Figure 3. PCM temperature in different areas of the accumulator during the first shutdown (discharging)*

247 As shown in Figure 3, the accumulator was fully charged at the beginning of the first shutdown
248 except for the edges where the temperature was above -7 °C. The temperature at the edges of the
249 accumulator is given by the two lateral thermocouples (S.T1) and (S.T2). This gap in the charging rate
250 is due to the current configuration and dimensions of the accumulator. The heat transfer is maximum

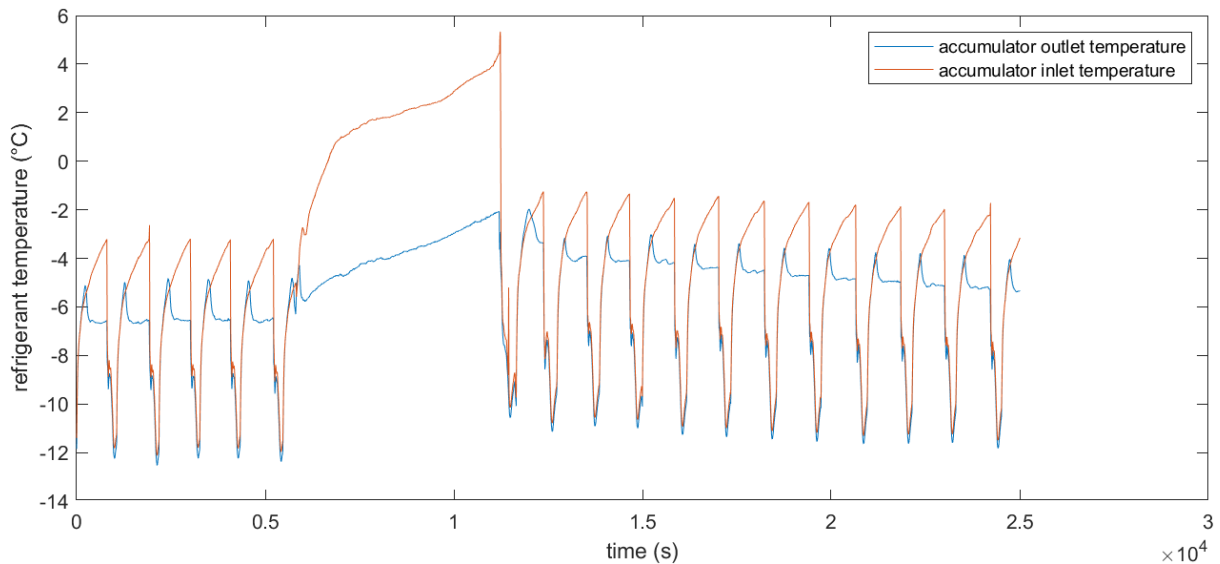
251 in the centre due to the circulation of the refrigerant in the heat exchanger tubes. Moreover, the size
252 of the fins does not allow an optimal transfer to the edges of the accumulator, resulting in a slow
253 charging rate of this area (data given by S.T2). During the compressor shutdown, the temperature of
254 the PCM rises because of the heat exchange between the refrigerant and the PCM (Figure 3). When
255 the thermosiphon effect is activated, the heat absorbed by the refrigerant from the products is
256 released into the accumulator. The accumulator then gradually discharges, transferring the
257 previously stored thermal energy (during the charging phase) to the refrigerant (Figure 4). This heat
258 transfer is shown in Figure 5.



259

260

Figure 4. Evolution of the charging rate of the accumulator per area during the first shutdown



261

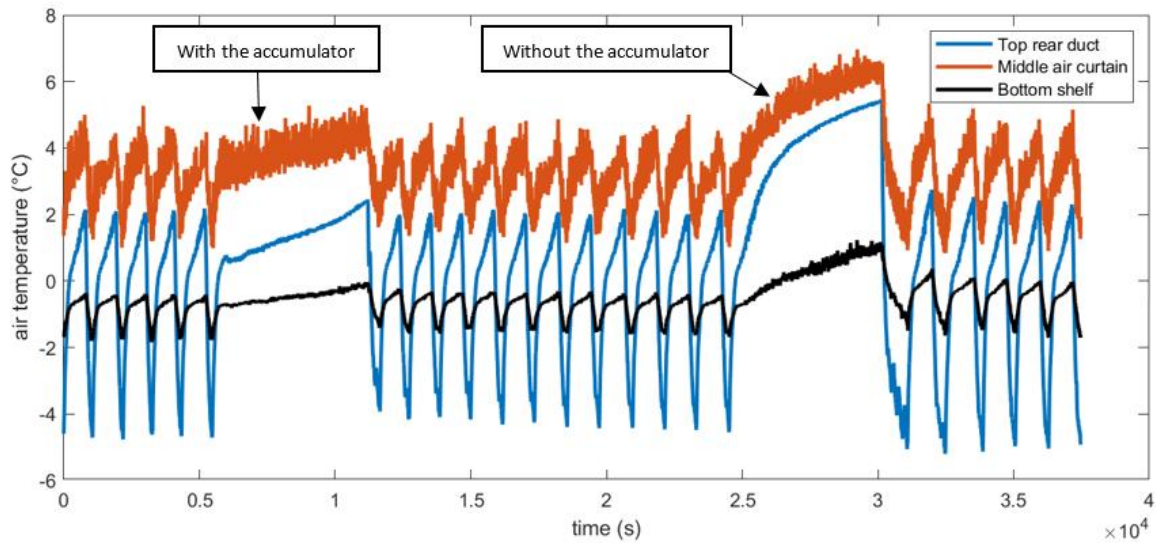
262 *Figure 5. Evolution of the refrigerant inlet and outlet temperatures at the accumulator during the first shutdown*

263 Before the compressor shutdown, the inlet and outlet temperatures of the refrigerant were
 264 approximately $-5\text{ °C} (\pm 2.43\text{ °C})$ and $-6\text{ °C} (\pm 1.91\text{ °C})$ respectively. At that time, the accumulator was
 265 fully charged and therefore there was little/no heat transfer between the refrigerant and the PCM.
 266 During the compressor shutdown, the temperature of the refrigerant entering the accumulator
 267 started to rise due to the absorption of heat from the cabinet products. The accumulator successfully
 268 lowers the refrigerant temperature from about $2\text{ °C} (\pm 1.42\text{ °C})$ to about $-4\text{ °C} (\pm 0.81\text{ °C})$, which is
 269 quite close to the refrigerant outlet temperature when the compressor is operating ($-6\text{ °C} \pm 1.91\text{ °C}$).
 270 After the compressor is restarted, it takes, on average, 98 minutes to charge the accumulator from 3
 271 % to 50 %. The accumulator takes longer to charge than to discharge because, during the charging
 272 phase, the cold transported by the refrigerant is shared between the accumulator and the display
 273 cabinet, whereas during the discharging phase, the refrigerant uses the cold stored in the
 274 accumulator to satisfy the needs of the entire cabinet.

275

276 **3.2 Air and products temperature evolution**

277 Figure 6 illustrates the evolution of the cabinet's air temperature during the two compressor
278 shutdowns in the rear duct, in the shelves and air curtain.



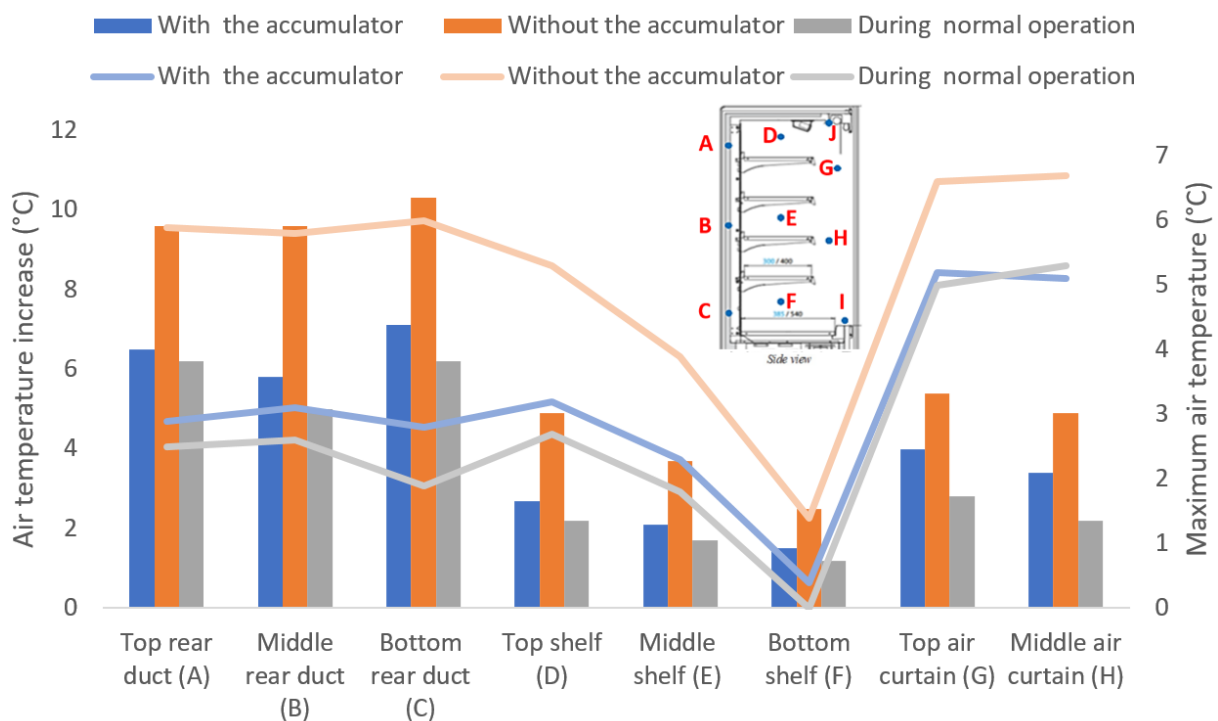
279

280

Figure 6. Evolution of the cabinet's air temperature during the two compressor shutdowns

281 During normal operation (between the two shutdowns), the air temperature varies because of the
282 compressor's on/off cycles. These variations are always less than 2.2 °C for the air temperature in the
283 rear duct, 2.3 °C for the air temperature in the shelves and 4.9 °C for the air temperature in the air
284 curtain. The significant disturbances observed for the air curtain temperature are due to the
285 influence of the ambient temperature, as the cabinet doors are not hermetically closed. The air
286 temperature rises more slowly during the first shutdown (with accumulator) than during the second
287 one (without the accumulator). In fact, during the first shutdown, the accumulator successfully
288 manages to keep the air temperature within the acceptable temperature range (normal operation)
289 for 72 minutes in the rear duct and 48 minutes in the shelves and the air curtain. However, during
290 the second shutdown (without the accumulator), it only takes 3 minutes, 5 minutes and 7 minutes,
291 respectively, for the air temperature to exceed the permissible temperature range in the rear duct, in
292 the shelves and in the air curtain. The air temperature rises rapidly without the accumulator because
293 no cooling is provided to the cabinet, which leads to heat build-up. The slow increase in the air
294 temperature with the accumulator is because cooling is provided to the cabinet due to the

295 accumulator discharging its cold energy through the thermosiphon effect. Figure 7 presents the
 296 increase in air temperature (histogram) and the maximum air temperature reached (line) in the rear
 297 duct, shelves and air curtain during the two compressor shutdowns and normal operation. The
 298 increase in air temperature was evaluated based on a reference temperature corresponding to the
 299 lowest temperature reached in normal operation for each position. The maximum increase in air
 300 temperature during normal operation is 6.2 °C compared with 7.1 °C when the compressor is shut
 301 down with the accumulator and 10.3 °C when the compressor is shut down without the accumulator.
 302 In the current configuration, for all positions, the accumulator slows the increase in air temperature
 303 but cannot stabilise it due to a lack of cooling power delivered towards the end of the shutdown
 304 time. However, it enables the cabinet to perform closer to normal operation. It is essential to note
 305 that the thermal inertia provided by the cabinet products also dampens the air temperature
 306 increase. If the percentage of the cabinet's storage volume occupied by the products were less than
 307 90 %, the increase would have been more significant for both cases (with and without accumulator).



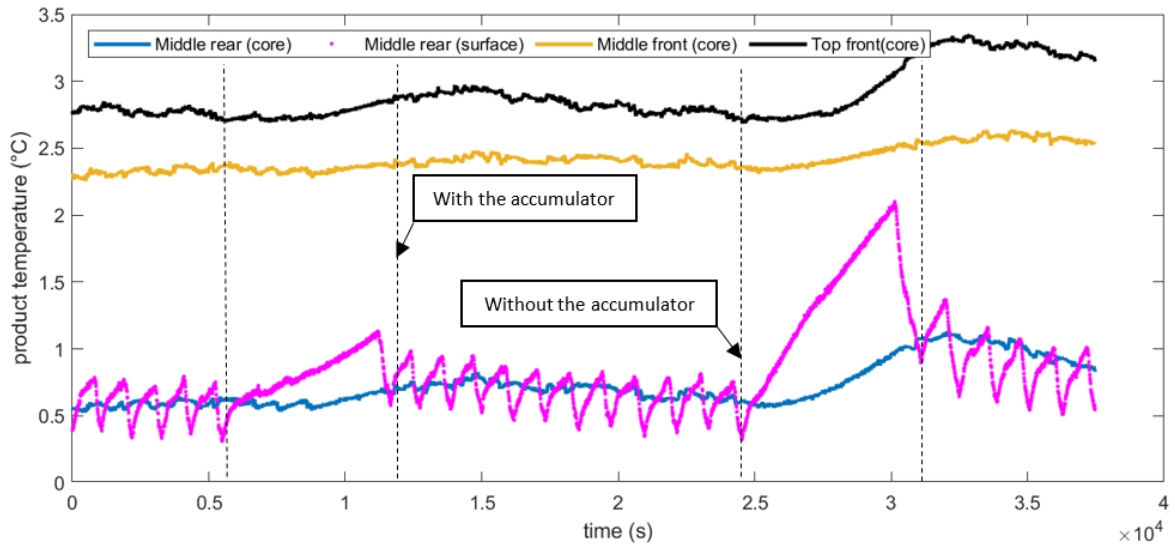
308

309 *Figure 7. Air temperature increase (histogram) and maximum air temperature (line) in the cabinet during the compressor*

310

shutdowns and normal operation

311 The temperature evolution of the products during the two shutdowns is presented in Figure 8. The
312 temperature variation between the shutdowns is due to the compressor on/off cycles during normal
313 operation.

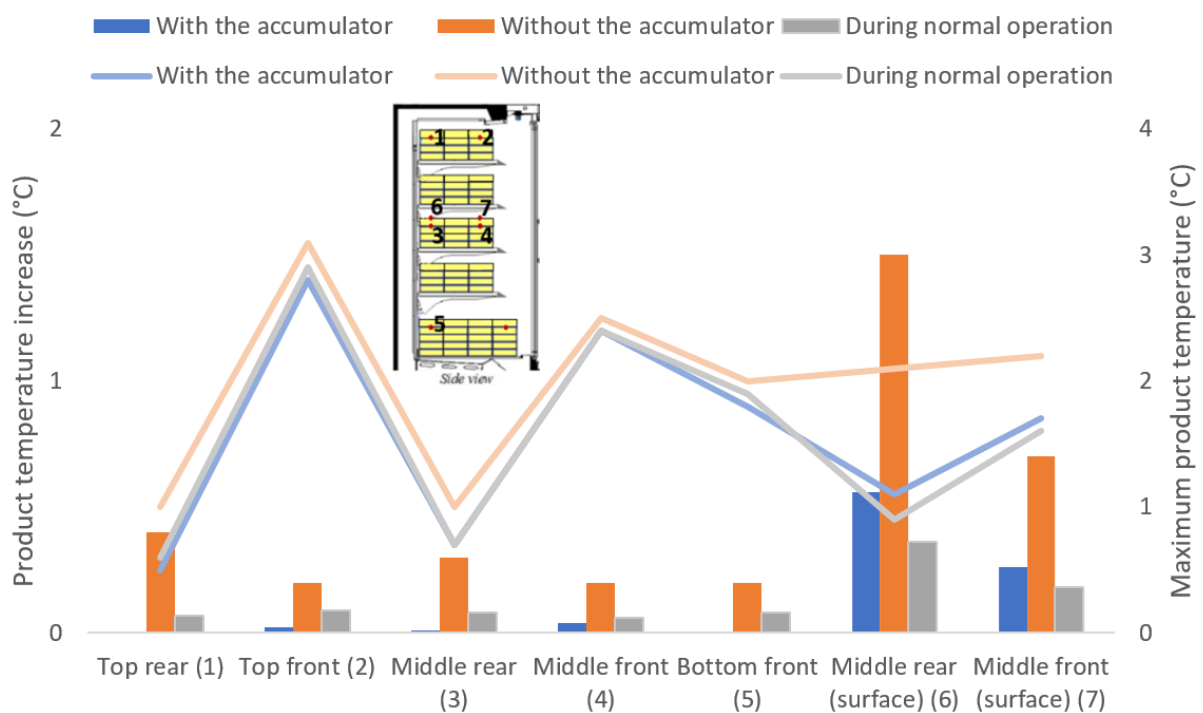


314

315

Figure 8. Evolution of the product temperature in the cabinet during the two compressor shutdowns

316 As expected, the temperature of the products rises more slowly during the shutdown with the
 317 accumulator than without the accumulator. The temperature of the products is affected differently
 318 depending on the products' position in the cabinet. The two compressor shutdowns had logically less
 319 impact on the products' core temperature than on the products' surface temperature, as shown by
 320 the different slopes, due to the thermal inertia acquired by the products during normal operation
 321 and because the surface of the products is the first part to be in contact with the (warmer) air.
 322 Products located at the rear are colder than products located at the front during normal operation
 323 and during the two shutdowns, as they are closest to the air distribution channels. Figure 9 presents
 324 the temperature rise (histogram) and maximum temperature reached (line) by the products
 325 depending on their position within the cabinet during compressor shutdowns and normal operation.



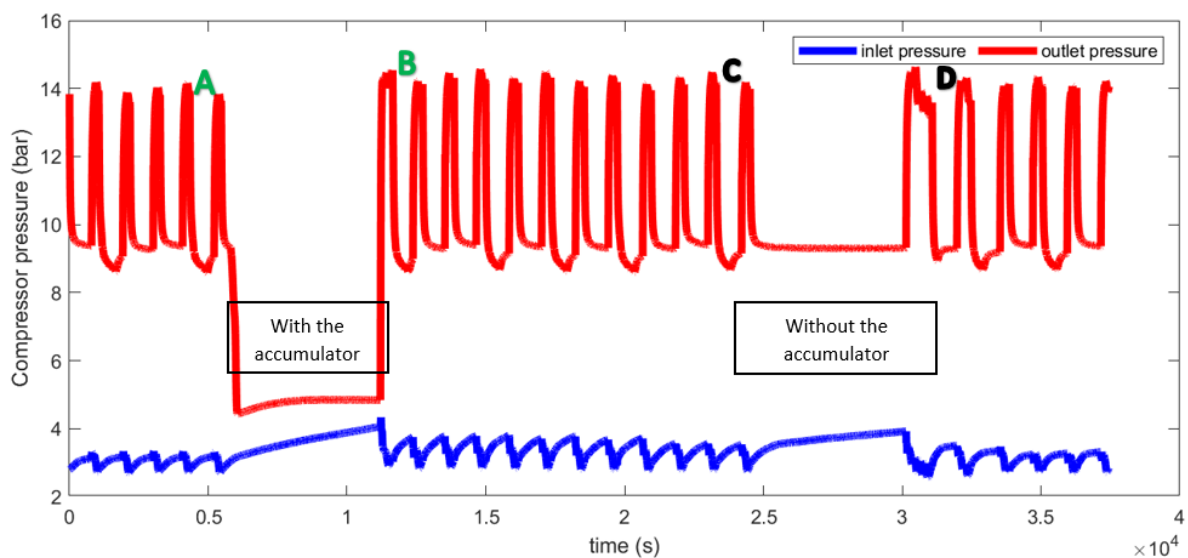
326
 327 *Figure 9. Increase in temperature (histogram) and maximum temperature (line) reached by the products depending on their*
 328 *position in the cabinet during compressor shutdowns and normal operation*

329 Discharging the accumulator during the first shutdown kept the core temperature of the products
 330 below the maximum temperature reached during normal operation. All increases in product
 331 temperatures were less than 0.6 °C. During the second shutdown (without the accumulator), the

332 product temperatures were maintained below the acceptable temperature for longer than the air
333 temperatures, thanks to the thermal inertia of the products. The longest holding time was 71
334 minutes (for the bottom products). The maximum increase observed in the case of the shutdown
335 without the accumulator was 1.5 °C. As the core of the products reacts slowly to air temperature
336 changes in the cabinet, after each shutdown (with and without the accumulator), when the
337 compressor has been restarted, the core temperature of the products continues to rise for a period
338 that depends on the position of the products in the cabinet, before decreasing. The cabinet's
339 temperature at the end of each shutdown affects the behaviour of the compressor when it is
340 switched on again.

341 3.3 Compressor behaviour

342 Figure 10 presents the pressure at the compressor inlet and outlet during the two shutdowns. The
343 on/off cycles responsible for the temperature variations in the accumulator, air and products during
344 normal operation are also illustrated.

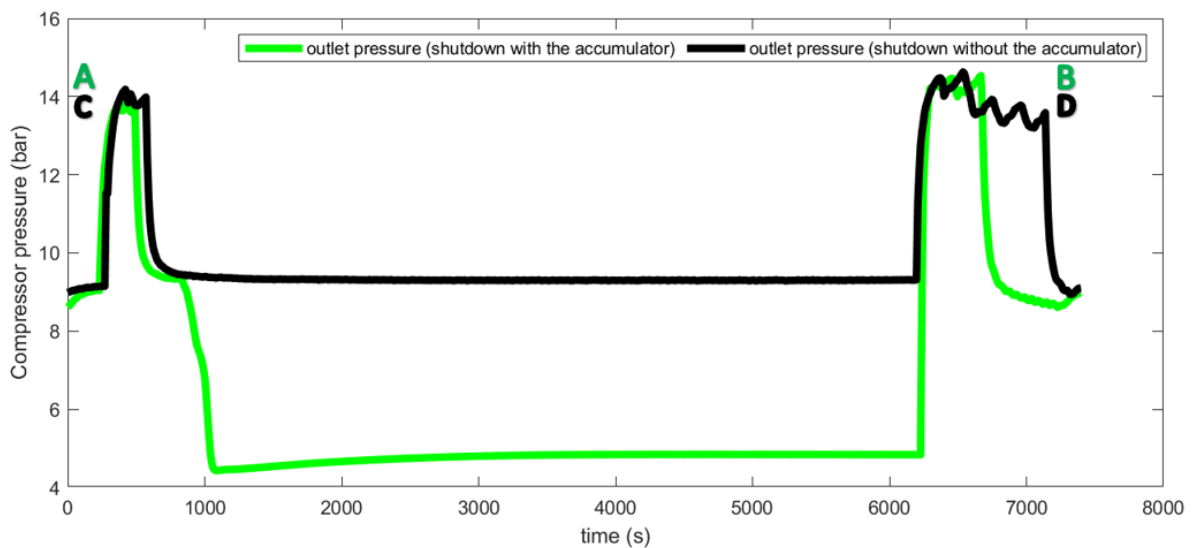


345

346 *Figure 10. Evolution of the compressor's inlet and outlet pressure during the two shutdowns*

347 During the shutdown with the accumulator, the compressor outlet pressure falls to the same level as
348 the inlet pressure due to the activation of the thermosiphon loop. In fact, in order to trap a sufficient

349 amount of refrigerant in the loop, when the compressor is shut down, the sensing bulb of the
350 thermostatic expansion valve (TXV) (Figure 1) triggers the opening of the TXV by heating up, which
351 considerably reduces the pressure in the compressor outlet channel. During the shutdown without
352 the accumulator, the outlet pressure at the compressor is the same as for a defrost period or an off
353 cycle because the TXV opening is not forced. When the compressor is restarted, the running time of
354 the compressor is longer after shutdown without the accumulator (about 931 s) than after shutdown
355 with the accumulator (about 430 s) (Figure 11). In the case of the shutdown without the
356 accumulator, the compressor runs longer to compensate for the high-temperature increase in the
357 cabinet (and therefore consumes more energy). In contrast, in the case of the shutdown with the
358 accumulator, the compressor runs less because the accumulator was able to reduce the temperature
359 rise in the cabinet during the shutdown (and therefore consumes less energy).



360

361

Figure 11. Evolution of the compressor's outlet pressure during the two shutdowns

362

363 4. Conclusion

364

This paper presents the working principle of a novel thermosiphon accumulator for cold storage

365

applications. The accumulator was designed to supply cold energy to the evaporator of any vapour

366 compression cycle machine during power cuts. It combines a phase change material to store thermal
367 energy and thermosiphon principle to release it. The ability of the accumulator to properly perform
368 its function as a cold provider was tested experimentally on the vapour compression cycle of a closed
369 refrigerated display cabinet. The compressor was shut down for 1.5 hours with and without the
370 accumulator. The temperature in the display cabinet and the accumulator, as well as the behaviour
371 of the compressor, were studied.

372 In summary, the heat transfer inside the accumulator is not homogeneous, and charging takes longer
373 than discharging (22 minutes to discharge from 89 % to 50 % compared with 98 minutes to charge
374 from 3 % to 50 %). Nevertheless, air and product temperatures rise slowly when the compressor is
375 shut down with the accumulator. The maximum increase in air and products temperatures with the
376 accumulator is 7.1 °C and 0.6 °C respectively, while without the accumulator, it is 10.3 °C and 1.5 °C
377 respectively. The compressor runs longer after the shutdown without the accumulator to reduce the
378 high-temperature rise in the cabinet. The accumulator can increase the lifespan of products in case
379 of sudden compressor breakdown. As long as enough energy is stored in the PCM, the system can
380 deliver it to the evaporator, thus promoting intermittent energies, demand side management, and
381 increasing product safety.

382 In further work, the internal design of the accumulator and the impact of operating parameters (such
383 as product loading, thermostat temperature, ambient temperature, and door opening) will be
384 studied in more detail, as they are thought to have an impact on the accumulator charging process
385 and the temperature rise in the cabinet, respectively. The energy consumption of the display cabinet
386 with the accumulator will also be assessed and compared to the energy consumption without the
387 accumulator.

388

389

REFERENCES

390 AHMED, M., MEADE, O. & MEDINA, M. A. 2010. Reducing heat transfer across the insulated walls of
391 refrigerated truck trailers by the application of phase change materials. *Energy Conversion*
392 *and Management*, 51, 383-392.

393 ALBERTSEN, B. & SCHMITZ, G. 2021. Experimental parameter studies on a two-phase loop
394 thermosyphon cooling system with R1233zd(E) and R1224yd(Z). *International Journal of*
395 *Refrigeration*, 131, 146-156.

396 ALZUWAID, F., GE, Y. T., TASSOU, S. A., RAEISI, A. & GOWREESUNKER, L. 2015. The novel use of phase
397 change materials in a refrigerated display cabinet: An experimental investigation. *Applied*
398 *Thermal Engineering*, 75, 770-778.

399 AZZOUZ, K., LEDUCQ, D. & GOBIN, D. 2009. Enhancing the performance of household refrigerators
400 with latent heat storage: An experimental investigation. *International Journal of*
401 *Refrigeration*, 32, 1634-1644.

402 BEN-ABDALLAH, R., LEDUCQ, D., HOANG, H. M., FOURNAISON, L., PATEAU, O., BALLOT-MIGUET, B. &
403 DELAHAYE, A. 2019. Experimental investigation of the use of PCM in an open display cabinet
404 for energy management purposes. *Energy Conversion and Management*, 198.

405 DONG, Y., COLEMAN, M. & MILLER, S. A. 2021. Greenhouse Gas Emissions from Air Conditioning and
406 Refrigeration Service Expansion in Developing Countries. *Annual Review of Environment and*
407 *Resources*, 46, 59-83.

408 DUPONT, J.-L., DOMANSKI, P., LEBRUN, P. & ZIEGLER, F. 2019. The role of refrigeration in the global
409 economy - 38 Informatory Note on Refrigeration Technologies. France.

410 FOSTER, A., CAMPBELL, R., DAVIES, T. & EVANS, J. 2013. A novel pcm thermo siphon defrost system
411 for a frozen retail display cabinet. *2nd IIR Conference on Sustainability and the Cold Chain*.
412 Paris.

413 FOSTER, A., CAMPBELL, R., DAVIES, T. & EVANS, J. 2015. *A novel passive defrost system for a frozen*
414 *retail display cabinet with a low evaporator. T.*

415 FU, W., LI, X., WU, X. & ZHANG, Z. 2015. Investigation of a long term passive cooling system using
416 two-phase thermosiphon loops for the nuclear reactor spent fuel pool. *Annals of Nuclear*
417 *Energy*, 85, 346-356.

418 HAWES, D. W., BANU, D. & FELDMAN, D. 1989. Latent heat storage in concrete. *Solar Energy*
419 *Materials*, 19, 335-348.

420 IEA 2018. The Future of Cooling: Opportunities for energy-efficient air conditioning. Paris: IEA.

421 LEE, S., KANG, H. & KIM, Y. 2009. Performance optimization of a hybrid cooler combining vapor
422 compression and natural circulation cycles. *International Journal of Refrigeration*, 32, 800-
423 808.

424 LEUNGTONGKUM, T., FLICK, D., HOANG, H. M., STEVEN, D., DELAHAYE, A. & LAGUERRE, O. 2022.
425 Insulated box and refrigerated equipment with PCM for food preservation: State of the art.
426 *Journal of Food Engineering*, 317, 110874.

427 LI, F., GAO, J., SHI, X., LIANG, F., ZHU, K. & LI, Y. 2018. Experimental investigation of an R600a two-
428 phase loop thermosiphon to cool a motorized spindle shaft. *International Communications in*
429 *Heat and Mass Transfer*, 97, 9-16.

430 LIU, M., SAMAN, W. & BRUNO, F. 2012. Development of a novel refrigeration system for refrigerated
431 trucks incorporating phase change material. *Applied Energy*, 92, 336-342.

432 LIU, W., CHEN, C., CAO, J., WU, L., REN, W., JIAO, D. & PEI, G. 2021. Experimental study of a novel
433 cool-storage refrigerator with controllable two-phase loop thermosiphon. *International*
434 *Journal of Refrigeration*, 129, 32-42.

435 MAIORINO, A., DEL DUCA, M. G., MOTA-BABILONI, A., GRECO, A. & APREA, C. 2019. The thermal
436 performances of a refrigerator incorporating a phase change material. *International Journal*
437 *of Refrigeration*, 100, 255-264.

438 MEMON, S. A. 2014. Phase change materials integrated in building walls: A state of the art review.
439 *Renewable and Sustainable Energy Reviews*, 31, 870-906.

440 ORÓ, E., MIRÓ, L., FARID, M. M. & CABEZA, L. F. 2012. Improving thermal performance of freezers
441 using phase change materials. *International Journal of Refrigeration*, 35, 984-991.

442 SOCACIU, L., PLESA, A., UNGURESAN, P. & GIURGIU, O. 2014. Review on phase change materials for
443 building applications. *Leonardo Electronic Journal of Practices and Technologies*, 13, 179-194.

444 SUTANTO, B., INDARTONO, Y. S., WIJAYANTA, A. T. & IACOVIDES, H. 2022. Enhancing the
445 performance of floating photovoltaic system by using thermosiphon cooling method:
446 Numerical and experimental analyses. *International Journal of Thermal Sciences*, 180,
447 107727.

448 TREWIN, R. R. 2021. Development of a one-dimensional model of a closed thermosiphon for cooling
449 a spent-fuel pool. *Nuclear Engineering and Design*, 374, 111027.

450 UNIDO 2020. Towards energy efficient retail refrigeration in developing countries. *In:*
451 ORGANIZATION, U. N. I. D. (ed.) *6th IIR International Conference on Sustainability and the*
452 *Cold Chain*. Nantes, France.

453 WANG, C., CHENG, C., JIN, T. & DONG, H. 2022. Water evaporation inspired biomass-based PCM from
454 daisy stem and paraffin for building temperature regulation. *Renewable Energy*, 194, 211-
455 219.

456 WANG, K., HU, C., CAI, Y., LI, Y. & TANG, D. 2023. Investigation of heat transfer and flow
457 characteristics in two-phase loop thermosyphon by visualization experiments and CFD
458 simulations. *International Journal of Heat and Mass Transfer*, 203, 123812.

459 YE, C., ZHENG, M. G., WANG, M. L., ZHANG, R. H. & XIONG, Z. Q. 2013. The design and simulation of a
460 new spent fuel pool passive cooling system. *Annals of Nuclear Energy*, 58, 124-131.

461 ZHANG, H., SHI, Z., LIU, K., SHAO, S., JIN, T. & TIAN, C. 2017. Experimental and numerical investigation
462 on a CO₂ loop thermosyphon for free cooling of data centers. *Applied Thermal Engineering*,
463 111, 1083-1090.

464 ZHANG, P., WANG, B., SHI, W., HAN, L. & LI, X. 2015. Modeling and performance analysis of a two-
465 phase thermosyphon loop with partially/fully liquid-filled downcomer. *International Journal*
466 *of Refrigeration*, 58, 172-185.